

Improvement of the physical properties of novel $(1 - x)$ $\text{CoFe}_2\text{O}_4 + (x)$ LaFeO_3 nanocomposites for technological applications

Ebtesam E. Ateia¹ · M. K. Abdelamksoud^{1,2} · M. A. Rizk¹

Received: 15 June 2017 / Accepted: 17 July 2017 / Published online: 1 August 2017
© Springer Science+Business Media, LLC 2017

Abstract Large leakage current and poor magnetization are the two biggest drawbacks of LaFeO_3 (LFO), which hinder the opportunities of its application in recent devices. On the other hand, CoFe_2O_4 (CFO) has remarkably high magnetic properties but its ferroelectric properties are lacking. An improvement of the multiferroic properties of LFO is a real challenge to the researchers' community. Nanocomposites are an excellent alternative in optimizing the physical properties of the blended species. We are aiming to enhance the properties of LFO/CFO nano-composites as compared to that of the individual perovskite and spinel phases. In this work, a composite system is established through physical mixing with different proportions. Phase formation has been checked using X-ray diffraction (XRD), and high resolution transmission electron microscopy (HRTEM). The energy dispersive X-ray spectroscopy plot reveals no extra peaks correlated to elements other than the constituents. The magnetic entropy change was estimated from magnetization data, using Maxwell relation. The other magnetic parameters are calculated for the different samples from the magnetic hysteresis loops. The obtained electric hysteresis loop of the critical composite is discussed. Significant improvement in the physical properties of 0.6LFO/0.4CFO nano-composite is achieved. This study of the combined perovskite–spinel nanostructures has shed some light on tailoring novel multiferroic materials with appreciably improved properties.

1 Introduction

Lanthanum ferrite (LFO) has typical antiferromagnetic character associated with weak ferromagnetization, lack of saturation and small area [1]. It has various promising applications in solid oxide fuel cells, catalysts, chemical sensors, etc. [2].

CoFe_2O_4 (CFO) shows some excellent physical properties such as, high resistivity chemical stability, reasonable saturation magnetization, high coercivity, large magnetic anisotropy and good mechanical [3]. However, studies that combine the perovskite LFO with a spinel system are very rare. This combination is a promising candidate for tailoring systems with outstanding multiferroic properties [4]. Multiferroics are important class of novel materials with coupled magnetic, electric, and structural order factors that produce simultaneous effects of ferro-magnetism, ferro-elasticity and ferro-electricity [5]. These investigations attract much attention because of their promising applications in data-storage media, spintronic devices, multiple-stage memories and sensors [6–8].

In this study, a new type of multiferroic perovskite and magnetic spinel based nano-composite, is synthesized. Each of LaFeO_3 and CoFe_2O_4 are prepared separately via a citrate auto combustion method, then the two phases are physically mixed. The main target is to study the improvement in magnetization and other physical properties when the perovskite LaFeO_3 combines with a spinel phase.

2 Experimental work

Spinel–perovskite nano-composites of $(1 - x)$ $\text{CoFe}_2\text{O}_4 + (x)$ LaFeO_3 with x values taken as 0.0, 0.2, 0.4, 0.6, 0.8 and 1.0 were synthesized by citrate auto combustion method.

✉ M. A. Rizk
mrizk822@gmail.com

¹ Physics Department, Faculty of Science, Cairo University, Giza 12613, Egypt

² Egypt Nanotechnology Center (EGNC), Cairo University, El-Sheikh Zayed 12588, Egypt

Stoichiometric amounts of metal nitrates and fuel (citric acid) are dissolved in distilled water. The pH is adjusted to seven using drops of ammonium hydroxide. The solution is then put on a hot plate and allowed to evaporate thoroughly. Finally, auto-combustion occurs and the required ferrite is formed. All ingredients were taken on the basis of analytical grade, $\text{Fe}(\text{NO}_3)_3 \cdot 9\text{H}_2\text{O}$ (ferric nitrate), $\text{LaN}_3\text{O}_9 \cdot 6\text{H}_2\text{O}$ and $\text{Co}(\text{NO}_3)_2 \cdot 6\text{H}_2\text{O}$. The citric acid was used to enhance the homogeneous mixing. The powder of CoFe_2O_4 were calcined at 600°C for 2 h with heating rate of $4^\circ\text{C}/\text{min}$. Structural characterization and particle morphology study of the prepared samples were tested using XRD by monochromatic $\text{Cu K}\alpha$ radiation and HRTEM respectively. The magnetization M (emu/g) as a function of the applied magnetic field intensity was measured at room temperature using a vibrating sample magnetometer (VSM) Model Lake Shore 7410. The polarization P was measured at room temperature as a function of electric field E using a homemade Sawyer–Tower circuit.

3 Results and discussion

The formation of CFO/LFO nano composite is established by their characteristic powder X-ray diffraction pattern as shown in Fig. 1. The diffraction peaks for the investigated samples correspond to spinel lattice with a cubic structure for CoFe_2O_4 and to perovskite orthorhombic structure for LaFeO_3 as compared and indexed with ICDD card numbers (01-078-4451) and (04-013-6775) respectively. No extra reflection peaks are detected in the X-ray diffraction patterns corresponding to any impurity phase. The obtained data also indicates that, there is no mixing phase between the two constituents of the nano-composite powders. This means a little inter diffusion occurs between the spinel and perovskite phases in the nano-composite powders.

Generally, the comparative sizes of the A and B cations are essential for the symmetrical [9] and thermodynamic stability [10] of the obtained structure. It can be identified for LFO by the Goldschmidt tolerance factor as shown in the following equation [11].

$$t = \frac{r_A + r_O}{\sqrt{2}(r_B + r_O)} \quad (1)$$

while the tolerance factor, T , for CFO spinel structure is calculated according to Roderick et al. [12] from the following equation:

$$T = \frac{1}{\sqrt{3}} \left(\frac{r_A + R_o}{r_B + R_o} \right) + \frac{1}{\sqrt{2}} \left(\frac{R_o}{r_B + R_o} \right) \quad (2)$$

where r_A , r_B and r_O are the ionic radii of the A, B cations and the oxygen anion respectively. For an ideal cubic perovskite structure the corresponding tolerance factor $t=1$.

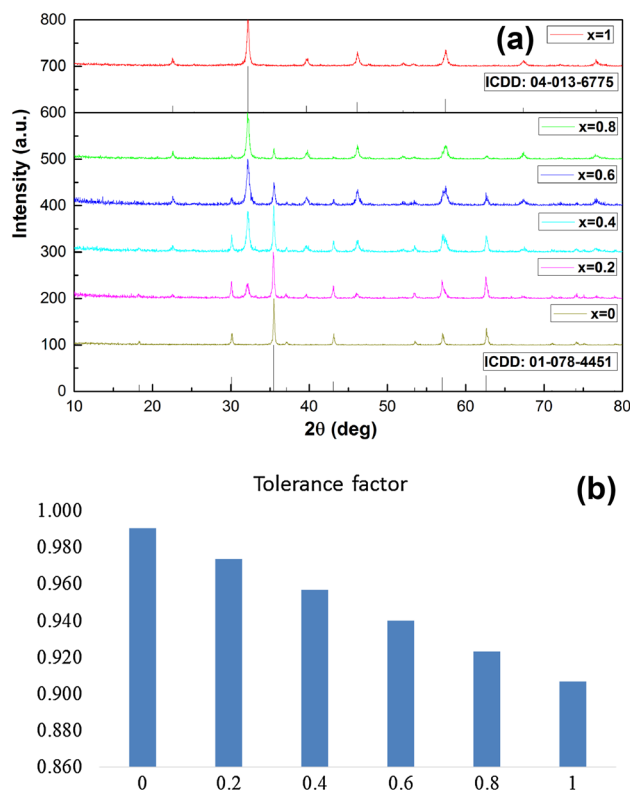


Fig. 1 **a** X-ray diffraction patterns, **b** the tolerance factor of the samples $(1-x)$ (CoFe_2O_4) + (x) (LaFeO_3) ($0 \leq x \leq 1$)

In our case as shown in Table 1, $t \approx 0.9$ and XRD gives orthorhombic distortion of the LFO structure. Moreover for CFO nano ferrites, we find a value of $T \approx 0.99$ suggesting defect free formation of spinel structure. The increase of La content results in a further structural distortion that affects the super exchange interactions of Fe-O-Fe . This distortion can suppress the spiral spin structure and decreases the magnetic properties which agree well with the obtained magnetic data as will be discussed later on.

Average crystallite size, experimental lattice parameter, and tolerance factor (t , T) of the nano-composites are calculated and tabulated in Table 1. The analysis of the crystallite size is carried out using the FWHM of the maximum intense peak corresponding to (112), (311) planes of the LFO and CFO respectively. The broadening of the peaks designates that the prepared nano composites crystallize in a nanosized scale.

The crystallite size of any of the constituents in the nano-composites is generally smaller than that of the individual parent. On the other hand, the lattice parameters of any of the constituents in the nano-composites are generally slightly bigger than that of the separate parent. These two observations may lead one to conclude that the two phases in the nano-composite are exposed to stress which will definitely affect the physical properties of the samples.

Table 1 The average crystallite size and the lattice parameter and tolerance factor for $(1-x)$ $(\text{CoFe}_2\text{O}_4) + (x)$ (LaFeO_3) ($0 \leq x \leq 1$)

x	Average crystallite size		Lattice parameters			Tolerance factor	
	CoFe ₂ O ₄ (nm)	LaFeO ₃ (nm)	CFO (Cubic) a = b = c (nm)	LFO (Orthorhombic)			
				a (nm)	b (nm)		c (nm)
0	38.698	–	0.838	–	–	–	0.991
0.2	32.209	19.347	0.839	0.557	0.559	0.789	0.974
0.4	32.790	19.056	0.839	0.557	0.555	0.786	0.957
0.6	29.451	17.134	0.839	0.556	0.557	0.786	0.940
0.8	40.527	19.679	0.840	0.556	0.556	0.787	0.923
1	–	21.638	–	0.556	0.555	0.787	0.906

Figure 2a–f illustrates the high resolution transmission electron microscopy (HRTEM) for the two parents and 0.6LFO/0.4CFO samples together with the selected area electron diffraction patterns (SAED). The grain shape of CFO sample is roughly spherical and highly agglomerated. In contrast the grain of LFO sample has little agglomeration and consists of platelets. As shown in Fig. 2b the two separate phases have a homogeneous distribution indicating a good physical mixing of the two phases. Figure 2d, e, f shows the size distribution of the studied samples and the average particle sizes are in the range of 30–50 nm. The particle size obtained from XRD line broadening agrees well with the particle size seen on the HRTEM images. Inset of Fig. 2 reveals the SAED pattern, which are the reflections of the spinel phase of CFO and perovskite phase of LFO. The diffuse diffraction spots ratify the nano-size of the studied samples.

The energy dispersive X-ray spectroscopy (EDAX) analyses of CFO, LFO and 0.6LFO/0.4CFO are shown in the Figure 3a–c. The EDAX plot reveals no extra peaks correlated to elements other than the constituents. All the composites show the exact match for standard peak position for La, Fe, Co and Oxygen. This reveals that the elemental composition of all the nano-composites does not contain any foreign elements.

The atomic percentage (at.%) and weight percentage (wt%) of constituent elements (Co, La, Fe and O) are calculated theoretically from the given formula CoFe_2O_4 and LaFeO_3 . The obtained data from EDAX elemental analysis is presented as inset of the figure. The difference between the expected weight percentage and the starting stoichiometric ratio of the studied samples can be attributed to many parameters. The most significant are the time constant (Tc), acceleration voltage (AV), dead time (DT), acquisition time (AT), and work distance (WD) which have direct effect on the energy resolution, natural width of characteristic X-ray lines and peak intensity [13].

The molar magnetic susceptibility with the absolute temperature for the nano ferrite samples at constant magnetic field intensity (1340 Oe) is shown in Fig. 4. It is clear

that, the magnetization increases slightly reaching a hump, this increase will continue until the thermal agitation will overcome the field effect and a drop of the magnetization with temperature is observed. This is a well known trend and it was previously discussed [14].

The inset of the curve is the first derivative of magnetization dM/dT to depict the accurate value of the Curie temperature T_C and tabulated in Table 2.

The obtained data obeys the well known Curie–Weiss law where χ_m varies linearly with temperature in the paramagnetic region. The values of the Curie constant, Curie Weiss constant and the effective magnetic moment are determined from the reciprocal of magnetic susceptibility with absolute temperature (not present here) as mentioned in the previous work [15]. The obtained data is summarized in the table.

The table shows that the Neel temperature T_N of LaFeO_3 is at ≈ 823 K. However, the T_N is shifted to a lower temperature at about 793 K for the 0.6LFO/0.4CFO composite. The change in the transition temperature of the LFO/CFO nano-composites can be attributed to (i) the lattice mismatch between both cubic and orthorhombic lattice parameters which induces mechanical strain at the interface between the CFO and LFO phases. And (ii) the super-exchange interaction between antiferromagnetic coupled Fe^{3+} ions in LFO that are debilitated due to the CFO phase. As shown from the Table, Θ is lower than T_C for $0.6 \leq x \leq 1.0$; which indicates the existence of weak antiferromagnetic interactions [16, 17].

Figure 5 shows the hysteresis loops of the investigated nano-composites using a vibrating sample magnetometer (VSM) with the applied field at 300 K. From the figure, it is clear that the magnetization increases with the applied magnetic field until reaching saturation point. A weak ferromagnetic nature with very small remanent magnetization is observed for LaFeO_3 ($M_r \approx 0.293$ emu/g). Actually, LFO possesses AFM with canted Fe^{3+} spins [18]. The weak ferromagnetism is due to partial alignment of the canted Fe^{3+} spins. The same magnetic behavior for LFO was previously observed [19]. On the other hand CoFe_2O_4 exhibits a

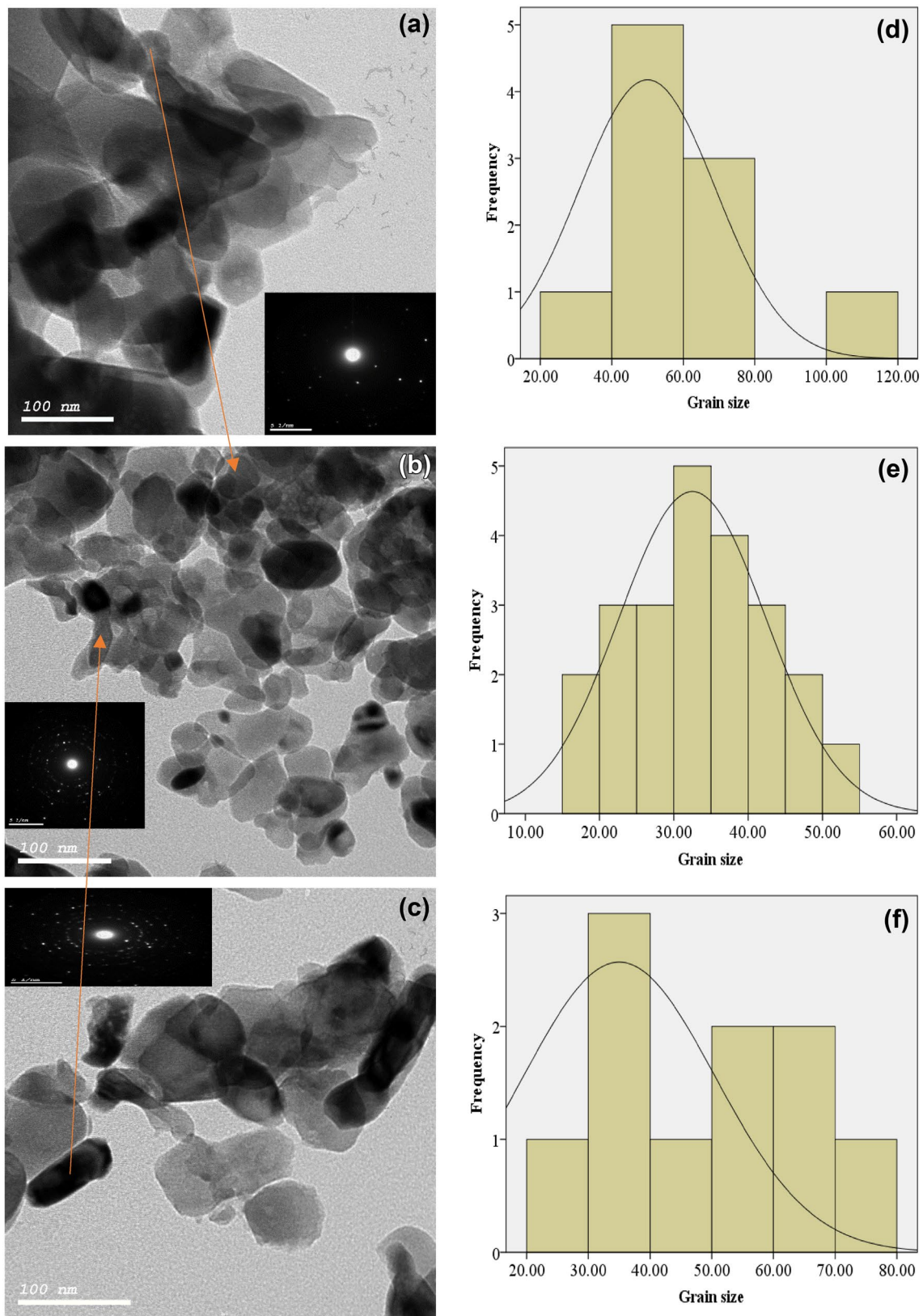
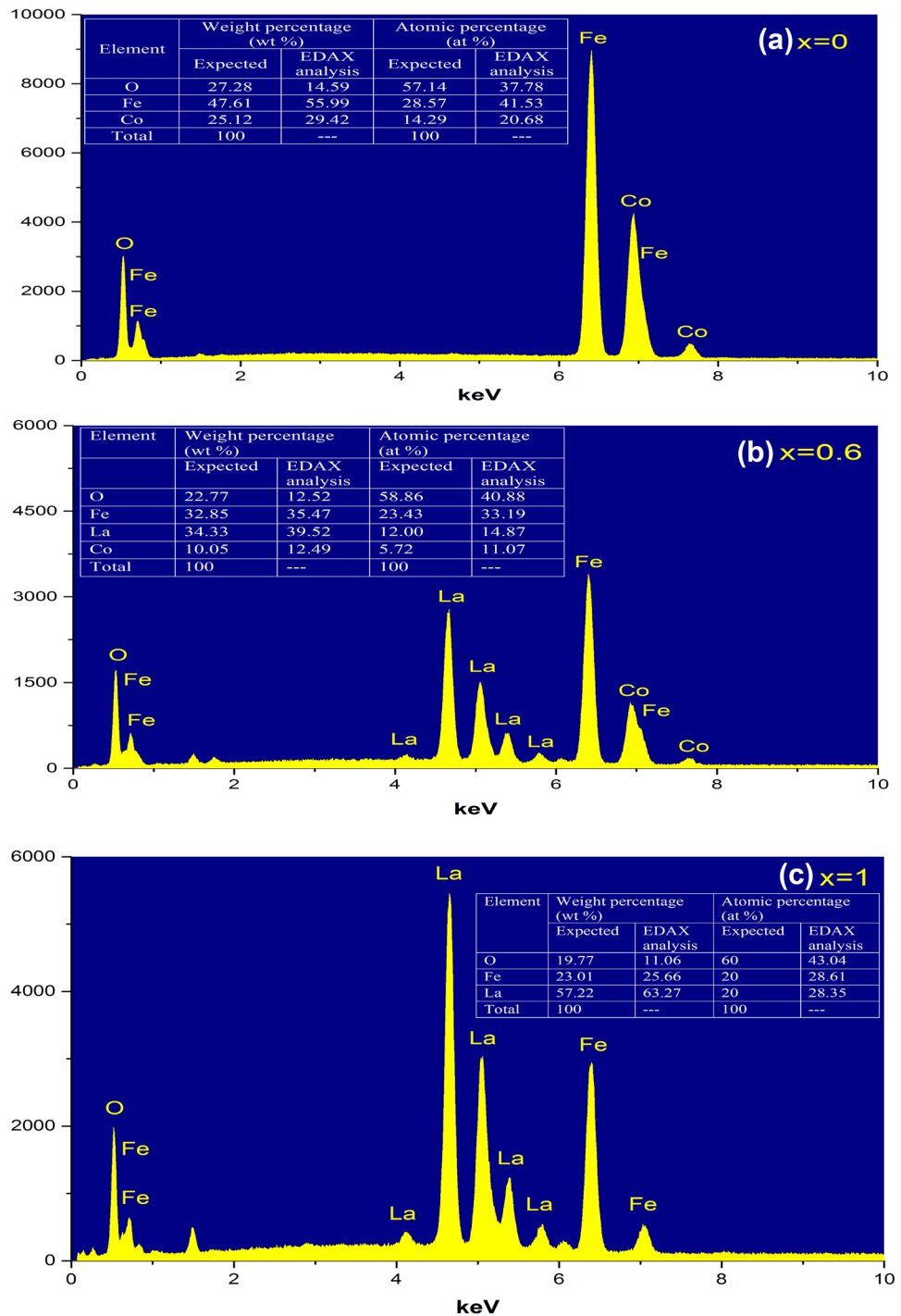


Fig. 2 The high resolution transmission electron microscopy (HRTEM) images and the SAED of **a** CoFe₂O₄, **b** 0.6LFO/0.4CFO and **c** LaFeO₃ nanoferrites. **d–f** The respective size distributions

Fig. 3 The energy dispersive X-ray spectroscopy (EDAX) analyses of **a** CFO ($x=0$), **b** 0.6LFO/0.4CFO ($x=0.6$) and **c** LFO ($x=1$)



typical ferromagnetic behavior, with a large saturation magnetization ($M_s=70.5$ emu/g). From the hysteresis loops, the coercivity (H_C), saturation magnetization (M_S), remnant magnetization (M_r), squareness (M_r/M_s) and anisotropy constant (K) are calculated and presented in Table 3.

The existence or absence of the numerous types of inter grain group exchanges is detected by the value of M_r/M_s that varies from 0 to 1 [20]. For the case study (M_r/M_s)

<0.5 this means that, the particle interact by magneto static interactions. The value of anisotropy constant K is determined using the following equation [21] and the obtained data is summarized in the Table

$$H_C = 0.98 K/M_S \tag{3}$$

The value of anisotropy constant for the critical composition $x=0.6$ ($K \approx 52$ emu Oe/g) is almost 150 times greater

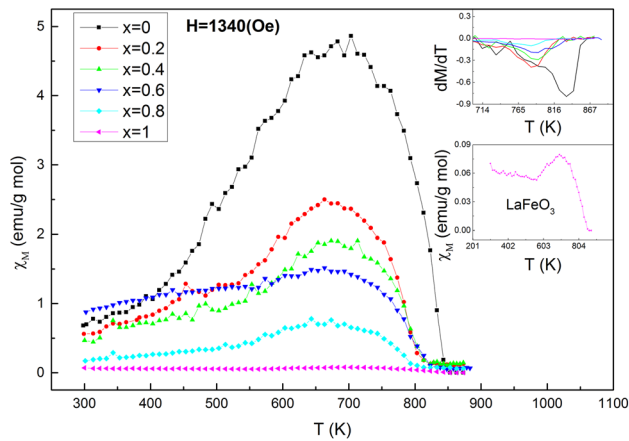


Fig. 4 Correlates the molar magnetic susceptibility with the absolute temperature for $(1-x)$ $\text{CoFe}_2\text{O}_4 + (x)$ LaFeO_3 ($0 \leq x \leq 1$) nano ferrite samples at constant magnetic field intensity (1340 Oe). The inset of the curve is the first derivative of magnetization dM/dT with temperature

Table 2 The Curie constant (C), Curie–Weiss constant (Θ), effective magnetic moment μ_{eff} and Curie temperature for the studied samples at constant field (1340 Oe)

x	Θ (K)	C (emu/gm mole) K	T_c (K)	T_c (entropy)	μ_{eff} (BM)
0	830.56	2.395	833.15	823.15	4.380
0.2	784.044	5.388	783.15	803.15	6.569
0.4	789.248	4.396	793.15	783.15	5.934
0.6	785.225	4.247	793.15	783.15	5.832
0.8	770.082	3.293	783.15	783.15	5.135
1	812.292	0.270	823.15	823.15	1.471

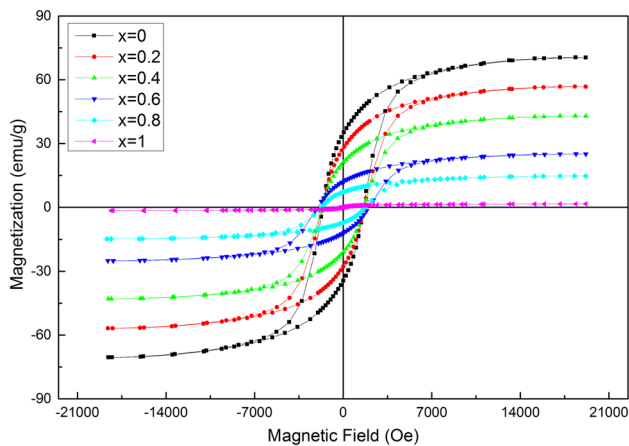


Fig. 5 The Vibrating sample magnetometer (VSM) hysteresis loops of $(1-x)$ $(\text{CoFe}_2\text{O}_4) + (x)$ (LaFeO_3) ($0 \leq x \leq 1$)

than anisotropy of lanthanum. This means that, the magnetization of the critical nano composite sample is in the hard direction rather than that of LFO along the easy direction.

The obtained data indicates that increasing Lanthanum nanoferrite content in the nanocomposites decreases the hysteresis loop area as well as all magnetic parameters, as expected. The only exception is the coercivity which shows a peak at the critical composition. The drop in almost all the magnetic parameters can be attributed to the increase in antiferromagnetic interaction between the La nano grains and the spinel ones.

Another important issue is the ferroelectric grains of LaFeO_3 that separate magnetic grains of the ferromagnetic phase leading to weakening of the exchange interaction. At higher lanthanum content, the ferroelectric grains become majority and will be treated as predominant phase in the nano composites.

The magnetic entropy change $\Delta S_M(T, H)$ is estimated from magnetization data by using Maxwell relation [22]. However, the maximum magnetic entropy change, is achieved at the Curie temperature where the ferromagnetic–paramagnetic phase transition takes place. The magnetic entropy data as a function of temperature for the studied samples is illustrated in Fig. 6. The calculated T_c from the Curie–Weiss law and the maximum entropy change are in good agreement, as shown in Table 2.

$$\Delta S_M(T, H) = \int_0^H \left(\frac{\partial M}{\partial T} \right)_H dH \quad (4)$$

Figure 7 illustrates the electric hysteresis loop of the 0.6LFO/0.4CFO nano-composite. The obtained data indicates that the electric hysteresis loop does not achieve saturation. The coexistence of spinel–perovskite phases causes the instability of the polarization states and promotes the rotation of polarization vector under external electric fields [23]. However, the presence of CoFe_2O_4 leads to lower resistance ratio of the sample and reduces the electric voltage, so that the nano composite is not fully polarized.

The saturation polarization (P_s), remnant polarization (P_r) and coercive field (E_c) for critical nano composite are $0.804 \times 10^{-2} \mu\text{C}/\text{cm}^2$, $0.697 \times 10^{-2} \mu\text{C}/\text{cm}^2$ and $9.923 \text{ V}/\text{cm}$, respectively. Similar behavior has been reported by Acharya et al. [24].

4 Conclusion

1. The average crystallite sizes of the investigated nano composite samples are in the range of ≈ 19 – 40 nm .
2. The obtained Curie temperature values from the Curie–Weiss law and the maximum entropy change are in good agreement with each other.

Table 3 The saturation magnetization, remnant magnetization, coercive field, squareness ratio, anisotropy constant and loop area for $(1-x)$ $(\text{CoFe}_2\text{O}_4) + (x)$ (LaFeO_3) ($0 \leq x \leq 1$)

x	H_c (Oe)	M_s (emu/g)	M_r (emu/g)	Squareness ratio M_r/M_s	Anisotropy (K) (10^3) (emu Oe/g)	Loop area (erg/g) 10^4
0	1615	70.5	34.513	0.490	116.203	32.2
0.2	1656	56.801	27.793	0.489	95.994	27.4
0.4	1667	42.965	21.024	0.489	73.093	20.7
0.6	2018	25.062	12.103	0.483	51.612	13.9
0.8	1734	14.745	7.189	0.488	26.085	7.3
1	210	1.594	0.293	0.184	0.342	0.1

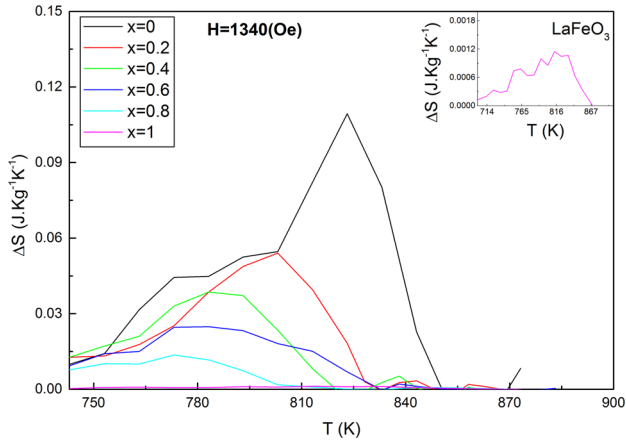


Fig. 6 The magnetic entropy change with the absolute temperature for $(1-x)$ $\text{CoFe}_2\text{O}_4 + (x)$ LaFeO_3 ($0 \leq x \leq 1$) nano ferrite samples at constant magnetic field intensity (1340 Oe) (smoothed by using Savitzky–Golay)

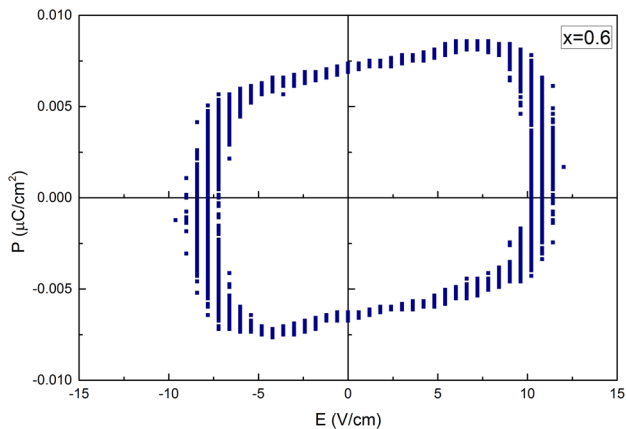


Fig. 7 The electric hysteresis loop of the 0.6LFO/0.4CFO nano composite

- The magnetic as well as the ferroelectric properties of the LFO/CFO nano-composites are enhanced.
- The promising candidate is 0.6LFO/0.4CFO nano-composite due to its relatively high coercivity, high saturated magnetization values and its good ferroelectric properties.

- The coercivity of the critical sample is enhanced by 1.25 times relative to the pure CFO.
- The investigated nano-composites seem to be valuable in data storage media.

References

- A.A. Azab, N. Helmy, S. Albaaj, Mater. Res. Bull **66**, 249 (2015)
- D. Wang, X. Chu, M. Gong, Nanotechnology **17**, 5501 (2006)
- E.E. Ateia, A.A. El-Bassuony, G. Abdelatif, F.S. Soliman, J. Mater. Sci. Mater. Electron. **28**, 241 (2017)
- J. Hoffmann, S. Schnittger, J. Norpöth, S. Raabe, T. Kramer, C. Jooss, J. Mater. Res. **27**, 1462 (2012)
- E. Salje, Ferroelectrics **104**, 111 (1990)
- J.F. Scott, Nat. Mater. **6**, 256 (2007)
- N.A. Hill, J. Phys. Chem. B. **104**, 6694–6709 (2000)
- M. Bibes, A. Barthélémy, Nat. Mater. **7**, 425 (2008)
- M. Johnsson, P. Lemmens, M. Johnsson, P. Lemmens, in *Handbook Magnetic Advanced Magnetic Materials* (Wiley, Chichester, 2007)
- J. Lian, K.B. Helean, B.J. Kennedy, L.M. Wang, A. Navrotsky, R.C. Ewing, J. Phys. Chem. B **110**, 2343 (2006)
- V.M. Goldschmidt, Naturwissenschaften **14**, 477 (1926)
- R.J. Hill, J.R. Craig, G.V. Gibbs, Phys. Chem. Miner. **4**, 317 (1979)
- D.E. Newbury, D.C. Joy, P. Echlin, C.E. Fiori, J.I. Goldstein, *Advanced Scanning Electron Microscopy and X-Ray Microanalysis*. (Plenum Press, New York, 1986)
- M.A. Ahmed, S.F. Mansour, M.A. Abdo, Mater. Res. Bull **48**, 1796 (2013)
- E.E. Ateia, G. Abdelatif, M.A. Ahmed, M.A. Alla Mahmoud, J. Supercond. Nov. Magn. **1**, 1–6 (2017)
- T. Dietl, H. Ohno, F. Matsukura, J. Cibert, D. Ferrand, Science **287**, 1019 (2000)
- A.M. Durand, D.P. Belanger, F. Ye, S. Chi, J.A. Fernandez-Baca, C.H. Booth, M. Bhat, Magnetism in nanoparticle LaCoO3 (2013), <http://arxiv.org/abs/1311.0240>
- M.A. Ahmed, N. Okasha, B. Hussein, J. Magn. Magn. Mater. **324**, 2349 (2012)
- M.B. Bellakki, V. Manivannan, P. McCurdy, S. Kohli, J. Rare Earths **27**, 691 (2009)
- A. Ghasemi, Ceram. Int. **42**, 4143 (2016)
- B.D. Cullity, in *Introduction to Magnetic Materials* (Addison-Wesley, Reading, MA, 1972), p. 233
- A.M. Tishin, J. Magn. Magn. Mater. **316**, 351 (2007)
- H. Zheng, J. Wang, S.E. Lofland, Z. Ma, L. Mohaddes-Ardabili, T. Zhao, L. Salamanca-Riba, S.R. Shinde, S.B. Ogale, F. Bai, D. Viehland, Y. Jia, D.G. Schlom, M. Wuttig, A. Roytburd, R. Ramesh, Science **303**, 661–663 (2004)
- S. Acharya, J. Mondal, S. Ghosh, S.K. Roy, P.K. Chakrabarti, Mater. Lett. **64**, 415 (2010)